JPET Fast Forward. Published on July 20, 2006 as DOI: 10.1124/jpet.106.105874

JPET #105874

ENZYME- MEDIATED PROTEIN HAPTENATION OF DAPSONE AND SULFAMETHOXAZOLE IN HUMAN KERATINOCYTES – 2. EXPRESSION AND ROLE OF FLAVIN-CONTAINING MONOOXYGENASES AND PEROXIDASES

Piyush M. Vyas, Sanjoy Roychowdhury, Sevasti B. Koukouritaki, Ronald N. Hines, Sharon K. Krueger, David E. Williams, William M. Nauseef, Craig K. Svensson.

Division of Pharmaceutics (PMV, SR, CKS), College of Pharmacy, and Inflammation Program, Department of Internal Medicine, Carver College of Medicine (WMN), The University of Iowa and Veterans Administration Hospital, Iowa City, IA; Department of Pediatrics and Pharmacology & Toxicology (SBK, RNH), Medical College of Wisconsin and Children's Research Institute, Children's Hospital and Health Systems, Milwaukee, WI; Department of Environmental and Molecular Toxicology and The Linus Pauling Institute (SKK, DEW), Oregon State University, Corvallis, OR.

Running Title: Role of FMOs and peroxidases in protein haptenation in keratinocytes.

Corresponding Author:

Craig K. Svensson, Pharm.D., Ph.D.; Division of Pharmaceutics, College of Pharmacy, The University of Iowa, 115 S. Grand Avenue, S213 PHAR, Iowa City, IA 52242

Tel: (319) 335-8823; Fax: (319) 335-9349; Email: craig-svensson@uiowa.edu

Number of pages of text: 33

Tables: 0

Figures: 8

Number of references: 40

Number of words in abstract: 204

Words in introduction: 403

Words in discussion: 1182

Abbreviations: ABH – 4-aminobenzoicacid hydrazide; BSA – bovine serum albumin; CDR – cutaneous drug reactions; DAB – 3,3' – diaminobenzidine tetrahydrochloride; DDS – dapsone; D-NO – dapsone nitroso; D-NOH – dapsone hydroxylamine; FMO – Flavin-containing monooxygenase; HEK – human embryonic kidney -293 cells, KCZ – ketoconazole; LPO: lactoperoxidase; MMZ – methimazole; MPO – myeloperoxidase; NHEK – normal human epidermal keratinocytes; PCR – polymerase chain reaction; PBS – phosphate buffered saline; PRX – Peroxidase; RT – reverse transcriptase; RT-PCR – Reverse transcription polymerase chain reaction; SMX – sulfamethoxazole; S-NOH- sulfamethoxazole hydroxylamine; TPO – thyroid peroxidase; TBS – Tris buffered saline.

Recommended section assignment: Cellular and molecular

ABSTRACT

Arylamine compounds, such as sulfamethoxazole (SMX) and dapsone (DDS), are metabolized in epidermal keratinocytes to arylhydroxylamine metabolites that auto-oxidize to arylnitroso derivatives, which in turn bind to cellular proteins and can act as antigens/immunogens. Previous studies have demonstrated that neither cytochromes P450 nor cyclooxygenases mediate this bioactivation in normal human epidermal keratinocytes (NHEK). In this investigation, we demonstrated that methimazole (MMZ), a prototypical substrate of the flavin-containing monooxygenases (FMOs), attenuated the protein haptenation observed in NHEK exposed to SMX or DDS. In addition, recombinant FMO1 and FMO3 were able to bioactivate both SMX and DDS, resulting in covalent adduct formation. Western blot analysis confirmed the presence of FMO3 in NHEK, whereas FMO1 was not detectable. In addition to MMZ, 4-aminobenzoic acid hydrazide (ABH) also attenuated SMX- and DDS-dependent protein haptenation in NHEK. ABH did not alter the bioactivation of these drugs by recombinant FMO3, suggesting its inhibitory effect in NHEK was due to its known ability to inhibit peroxidases. Studies confirmed the presence of peroxidase activity in NHEK, however, immunoblot analysis and RT-PCR indicated that myeloperoxidase, lactoperoxidase and thyroid peroxidase were absent. Thus, our results suggest an important role for FMO3 and yet to be identified peroxidases in the bioactivation of sulfonamides in NHEK.

INTRODUCTION

Biotransformation of non-reactive drugs or chemicals to reactive intermediates or metabolites is believed to be an important step in the provocation of numerous adverse drug reactions, especially those that appear to be immune-mediated. Whereas the liver is the major site for the generation of reactive metabolites, organs other than the liver are often the primary or secondary target for toxicity. As the ability of unstable metabolites to distribute from the liver to other organs is questionable, it has been proposed that extrahepatic metabolism (e.g., in circulating cells) may be important in mediating such toxic events (Uetrecht, 1992).

Skin eruptions after systemic drug administration represent one of the most commonly reported adverse drug reactions. Many drugs associated with cutaneous drug reactions (CDRs) are known to be metabolized to reactive metabolites (Roychowdhury and Svensson, 2005). However, the survival of such metabolites during transit from liver to the skin is undocumented. We have suggested that bioactivation of drugs in the skin may play an important role in the initiation of CDRs (Reilly et al., 2000). Utilizing sulfonamides as model compounds to test this hypothesis, we have shown the bioactivation of sulfamethoxazole (SMX) and dapsone (DDS) to their respective arylhydroxylamine metabolites (S-NOH, D-NOH) in normal human epidermal keratinocytes (NHEK) (Reilly et al., 2000). Moreover, we have demonstrated that incubation of such cells with the parent compounds gives rise to protein haptenation (Roychowdhury et al., 2005).

Whereas the formation of the arylhydroxylamine metabolites of these compounds in the liver is mediated primarily via cytochromes P450 (Cribb et al., 1995; Mitra et al.,

1995; Winter et al., 2000), it is unclear what enzyme(s) bioactivate these drugs in NHEK. In the first of these two companion papers, we demonstrate that cytochromes P450 do not play a major role in the protein haptenation observed in NHEK exposed to SMX or DDS. In addition, though other investigators have reported that cyclooxygenase-2 is able to oxidize arylamine compounds (Goebel et al., 1999), our results indicate that neither cyclooxygenase-1 nor -2 is involved in the protein haptenation observed in these cells (Vyas et al., 2006). Hence, we probed the role of flavin-containing monooxygenases (FMOs) and peroxidases (PRXs) in this phenomenon. Our results indicate that FMOs and PRXs are the primary enzymes that bioactivate these drugs in NHEK and thereby generate haptenated proteins. Based on these findings extrapolation of observations in one organ of bioactivation to another (e.g., liver to skin) must be made cautiously.

METHODS

Materials. DDS, SMX, ketoconazole (KCZ), methimazole (MMZ), 4-aminobenzoic acid hydrazide (ABH), magnesium chloride, $NADP^+$, glucose-6-phosphate, glucose-6-phosphate dehydrogenase, 3, 3'-diaminobenzidine tetrahydrochloride (DAB), and rat tail collagen (type-I) were obtained from Sigma (St. Louis, MO). DDS and SMX hydroxylamine metabolites were synthesized as described previously (Vyas et al., 2005). Rabbit anti-sera was raised against SMX- and DDS-keyhole limpet hemocyanin conjugates and specificity assessed as described previously (Reilly et al., 2000). Normal human epidermal keratinocytes and keratinocyte culture media were obtained from CAMBREX (Walkersville, MD). Microtiter ELISA plates (96 well) were obtained from Rainin Instruments (Woburn, MA). Goat-anti-rabbit IgG conjugated with Alexafluor 488 and goat anti-rabbit antibody conjugated with alkaline phosphatase, Amplex red reagent and YoYo-1 were purchased from Molecular Probes (Eugene, OR). Mouse monoclonal antibody to human thyroid peroxidase (TPO) and rabbit polyclonal anti-mouse IgG antibody conjugated to alkaline phosphatase was purchased from Abcam (Cambridge, MA). Pure TPO was obtained from Fitzgerald Industries International, Inc. (Concord, MA). Human salivary gland mRNA, used as a positive control for lactoperoxidase (LPO), was obtained from Clontech (Mountain view, CA). A human promyelocytic cell line (PLB-985 cells) known to express myeloperoxidase (MPO) was obtained from Dr. Tom Redo (Tucker et al., 1987) and used as a positive control for MPO. Polyclonal antibodies raised against human FMO1 and FMO3 peptides and horseradish peroxidase-conjugated goat anti-rabbit IgG were obtained from Gentest (Woburn, MA). Protein molecular weight standards (bench mark prestained protein

ladder) were from Invitrogen (Carlsbad, CA). Donkey anti-rabbit – HRP antibody, nitrocellulose membranes and enhanced chemiluminescence Western blotting kits were purchased from Amersham Pharmacia Biotech (Arlington Heights, IL). The 1-step NBT/BCIP substrate, micro bicinchoninic acid protein assay and Bradford assay reagent were purchased from Pierce Chemical Company (Rockford, IL). Immunomount was obtained from Vector Laboratories (Burlingame, CA). The pCEL1001 plasmid containing the Celera 19600414014330 cDNA representing full-length human FMO1, position +61 to +2172 inserted into pCMVSport 6 at the *Spe*I site, Trizol reagent, TOPO cloning kits, and all reagents for baculovirus protein expression were purchased from Invitrogen (Carlsbad,CA). RNeasy and One-Step RT-PCR kits were obtained from Qiagen (Valencia, CA). Criterion precast acrylamide gels and the Criterion Gel Electrophoresis system were purchased from Bio-Rad (Hercules, CA). All other chemicals and reagents were purchased from Sigma (St. Louis, MO) or Fisher Scientific (Chicago, IL).

Cell Culture. Normal human epidermal keratinocytes (NHEK) cells were cultured as detailed previously (Reilly et al., 2000). In brief, cells were propagated in 75 cm^2 flasks using basal media (KBM-2) supplemented with bovine pituitary extract (7.5 mg/ml), human epidermal growth factor (0.1 ng/ml), insulin (5 μg/ml), hydrocortisone, (0.5 μg/ml), epinephrine, transferrin, gentamicin (50 μg/ml) and amphotericin B (50 ng/ml) (KGM-2) at 37°C in a humidified atmosphere containing 5% CO_2. Media was replaced every 2-3 days. When the cultures were nearly confluent (70-90%), cells were disaggregated using 0.025% trypsin/0.01% EDTA in HEPES buffer followed by neutralization with 2 volumes of trypsin neutralizing solution. Cell suspensions were then centrifuged at 220 x *g* for 5 min followed by washing in KBM-2 and re-suspension

JPET Fast Forward. Published on July 20, 2006 as DOI: 10.1124/jpet.106.105874
This article has not been copyedited and formatted. The final version may differ from this version.

in KGM-2. Cells were then either subcultured or cryo-preserved for further purposes. All experiments were performed using 3rd to 4th passage cells.

Determination of KCZ, MMZ and ABH Cytotoxicity in NHEK. To determine the maximal non-cytotoxic concentrations of KCZ, MMZ and ABH in NHEK to block the respective enzymes, the cytotoxicity of concentrations ranging from 25 μM to 25 mM was examined. Cytotoxicity was determined using an impermeable DNA binding dye (YoYo - 1), as we have described previously (Vyas et al., 2005).

ELISA Analysis of Drug/Metabolite-Protein Adducts. Formation of covalent adducts following SMX or DDS exposure, in the presence or absence of KCZ, MMZ or ABH, was determined by cultivating NHEK (1 X 10^6 cells) for 24 h in 50 ml centrifuge tubes containing 10 ml of complete growth medium. The caps of the tubes were slightly loosened to maintain the aerobic conditions. The concentrations of KCZ, MMZ and ABH used were the maximum non-cytotoxic concentrations determined in NHEK. Cells were then incubated with the compounds 3 h prior to or immediately before addition of SMX (1 mM ascorbic acid was added prior to the addition of SMX as we have previously reported that ascorbic acid increases the protein haptenation in NHEK (Roychowdhury et al., 2005)) or DDS treatment for 3 h (concentrations specified in Results). Following the total 6 h or 3 h incubation, tubes were centrifuged at 220 *g* for 5 min to pellet the cells. Covalent adducts were determined as previously described (Vyas et al., 2005).

Immunocytochemistry. Drug/metabolite-protein covalent adduct formation was also visualized using immunofluorescence confocal microscopy. Cells were grown on collagen-coated (0.1 mg/ml) coverslips placed in Petri-dishes containing 2 ml of complete growth medium. After 24 h, cultures were subjected to KCZ, MMZ or ABH for

3 h (maximum non-cytotoxic concentrations were used), followed by SMX or DDS treatment for 3 h (concentrations specified in Results). After the total 6 h incubation, cells were washed (three times) with phosphate buffered saline (PBS: 0.05M sodium phosphate, 0.15M NaCl, pH 7.4) and fixed for 20 min with 4% paraformaldehyde in PBS. After fixation, cultures were washed 3 times with PBS followed by blocking for 60 min with Tris-casein buffer containing 0.3% Triton X-100 and overnight incubation with the anti-DDS or anti-SMX antisera (1:500 diluted in blocking buffer) at 4^{o}C. Coverslips were then washed with PBS, incubated for 3 h at 37^{o}C with the fluorochrome-conjugated secondary antibody (Alexa fluor-488 labeled goat-anti-rabbit IgG, 1:500 diluted in blocking buffer), and mounted on glass slides using Immunomount® containing anti-fade reagent.

Fluorescence images were acquired with a Zeiss Laser Scanning Microscope (LSM 510, Zeiss Axiovert stand, Zeiss 63x and 20x objective lens) using excitation at 488 nm. Emission was set to a long pass filter at 505 nm.

Image Analysis. For confocal laser scanning microscopy; laser attenuation, pinhole diameter, photomultiplier sensitivity and offset were kept constant for every set of experiments. Images were acquired from 3 different view fields of each slide. The obtained images were quantitatively analyzed for changes in fluorescence intensities within regions of interests (boxes drawn over cell somata) using the Image J software (National Institutes of Health). Fluorescence values from a minimum of three view fields consisting of 15-20 NHEK cells in each field from three different slides of each treatment were averaged and expressed as mean ± SD fluorescence intensity.

Peroxidase Assay in NHEK. PRX activity was determined using the fluorescent dye, Amplex red. Briefly, $5x10^6$ NHEK cells were lysed in 0.5 ml of 10 mM sodium phosphate buffer (pH 7.4). The cell lysate was centrifuged at 2040 *g* for 2 min in a microcentrifuge to obtain the supernatant fraction. Protein content of the supernatant fraction was determined using Bradford assay. Various amount of protein of the supernatant fraction (10 µg – 50 µg) was mixed with 50 µM Amplex red reagent and 1 mM H_2O_2 in a microtiter plate and then incubated in the dark at room temperature for 1 h. Following the incubation period of 1 h, the reactions were read in a fluorescence plate reader (Cytofluor®) at an excitation wavelength of 530 nm and an emission wavelength of 580 nm. The PRX activity was determined by measuring the observed fluorescence intensity.

The presence of PRXs was also determined by mixing 300 µl of cell lysate supernatant with 0.27 mM of 3,3' – diaminobenzidine tetrahydrochloride (DAB) and 1.4 mM H_2O_2 in 100 mM potassium acetate buffer (pH 5.0) in a microtiter plate. Following incubation in the dark at room temperature for 24 h, absorbance at 450 nm was measured to assess the presence of PRXs in the NHEK cell lysate.

MPO Immunoblot Analysis. Lysates of NHEK or PLB-985 cells and purified MPO were solubilized in SDS sample buffer and separated by SDS-PAGE in 9% acrylamide gel. Immunoblots were probed with rabbit polyclonal antibody to human MPO (Nauseef et al., 1983) followed by secondary donkey anti-rabbit antibody conjugated to HRP (Amersham).

Reverse Transcription Polymerase Chain Reaction (RT-PCR) Amplification for MPO and LPO. Total RNA was isolated from human salivary glands, NHEK, PLB-985

and human embryonic kidney-293 (HEK) cells using a Qiagen RNeasy kit (Qiagen, Valencia, CA) following the manufacturer's protocol. cDNA was generated using 1750 ng total RNA in a synthesis reaction using Qiagen One Step reverse transcriptase (RT) with random hexamers according to the supplier's protocol. PCR amplification was performed using the MPO-specific forward primer, 5' – AAC ATC ACC ATC CGC AAC CAG AT - 3', and reverse primer, 5' – AAT GCA GGA AGT GTA CTG CAG TT - 3', resulting in a 1.2 kbp product, and the LPO specific forward primer, 5'-TCA TGC AG T GGG GTC AGA TTG TGG A-3', and reverse primer, 5'-CGG AAG GCG AAG GTG AAG ACA TTG G-3', resulting in a 744 bp product. PLB cells and human salivary glands were used as a positive control for MPO and LPO, respectively, and HEK cells were used as negative control for both reactions. GAPDH was used as housekeeping gene and was amplified from the keratinocyte cDNA using the primers 5'-CCA CCA CCC TGT TGC TGT AGC-3' and 5'-GGA TCC CCA CAG TCC ATG CCA-3' resulting in a 455 bp fragment. Amplifications were performed in 50 μl reactions. Cycling conditions for MPO and GAPDH consisted of an initial incubation at 50° for 30 min followed by denaturation at 95° for 15 min, then 25 cycles of 94° for 1 min, 53° for 30 s, and 72° for 2 min, and a final 72° extension for 10 min. Cycling conditions for LPO consisted of an initial incubation at 50° for 30 min followed by 37 cycles of 94° for 2.5 min, 68° for 30 s, and 72° for 1 min, and a final extension at 72° for 10 min. Reactions were analyzed on 0.7% agarose gels stained with ethidium bromide.

MPO Chlorination Assay. MPO-mediated hypochlorous acid formation was measured using a previously reported method for quantification of taurine chloramine (Kettle and Winterbourn, 1994). Briefly, 5 X 10^7 NHEK cells suspended in 10 ml Hanks balanced

JPET Fast Forward. Published on July 20, 2006 as DOI: 10.1124/jpet.106.105874
This article has not been copyedited and formatted. The final version may differ from this version.

salt solution (HBSS) without Ca^{+2} or Mg^{+2} were incubated with 1 mM of diisopropylfluorophosphate to inhibit endogenous serine proteases. Cells were washed, resuspended in 0.5 ml relaxation buffer (10 mM PIPES, 3 mM NaCl, 3.5 mM $MgCl_2$, 100 mM KCl at pH 7.3) containing 1 mM $ATP(Na)_2$, and cavitated in 350 psi N_2, as previously described for neutrophils (Borregaard et al., 1983). The cavitate was collected in relaxation buffer containing 1 mM EGTA and centrifuged at 200 *g* for 10 min to remove unbroken cells and nuclei. The postnuclear supernatant was centrifuged at 100,000 *g* x 20 minutes to obtain cytosol and membrane for subsequent study. Reaction buffer (Dulbecco's PBS + 20 mM taurine + 1 mM glucose) was added to cytosol and supernatant and one hundred µl of each were incubated at 37°C for 90 min in the presence or absence of a cell-free H_2O_2-generating system, composed of 10 mM acetaldehyde and 0.01 U of xanthine oxidase in reaction buffer. The reaction was terminated by adding 200 U of catalase and the reaction mixture was cooled on ice for 10 min prior to the addition of 1 mM 5-thio-2-nitrobenzoic acid (TNB, extinction coefficient = 14,100 /M/cm) and incubated for 5 min in the dark at room temperature. The absorbance was measured at 412 nm (A_{412}) to assess the concentration of TNB in solution and the hypochlorous acid produced was calculated by determining the loss in A_{412} of the sample without acetaldehyde compared to the A_{412} of the sample with acetaldehyde and dividing by 28200, the molar extinction coefficient for two moles of yellow TNB reacting with one mole of taurine chloramine to form one mole of colorless 5,5'-dithiobis(2-nitrobenzoic acid) (DTNB).

TPO Immunoblot Analysis. NHEK cell lysate (75 µg) and purified TPO were solubilized in SDS sample buffer and separated by PAGE in 10% SDS gel.

Immunoblots were probed with mouse monoclonal antibody to human TPO followed by secondary rabbit anti-mouse – alkaline phosphatase conjugated antibody. NBT/BCIP was used as substrate for the secondary antibody to determine the presence of TPO.

Expression of Human Recombinant FMO3 and FMO1. A baculovirus/insect cell system was used for cloning and expression of FMO3 and FMO1. FMO1 cDNA was amplified by PCR from pCEL1001 using the forward primer, 5'-CAC CAT GGC CAA GCG AGT TGC-3', and the reverse primer, 5'-TTT TAC TTA TAG GAA AAT CAG AAA AAT AG-3' (underlined sequences correspond to the start and stop codon positions in the forward and reverse primers, respectively). The resulting 1606 bp amplicon representing FMO1 sequences from +98 to +1703 (accession number NM_002021) was cloned into the pENTR/SD/D-TOPO plasmid using a TOPO cloning kit (Invitrogen).

The original full-length FMO3 cDNA was amplified from an adult liver RNA sample using RT-PCR and the forward primer, 5'-TTG GAC AGG ACG TAG ACA CA-3', and reverse primer, 5'-TGG GTA TTG TCA GTA ACT TTC A-3'. The resulting 1711 bp amplicon was cloned into the pCR2.1 vector using AT cloning, resulting in pRNH696.

To move the FMO3 cDNA into the pENTR shuttle vector, PCR amplification was performed using linearized pRNH696 as a template and the forward primer, 5'-CAC CAT GGG GAA GAA AGT G-3', and reverse primer, 5'-GAT GAT TAG GTC AAC ACA AG-3'. The resulting 1604 bp amplicon was then cloned into the pENTR/SD/D-TOPO plasmid using the TOPO cloning kit, The resulting cDNA clone, pRNH829, contains FMO3 sequences from position +91 to +1697 (accession number NM_001002294). For both the FMO1 and FMO3 shuttle vectors, the fidelity of the amplified products were verified by complete DNA sequence analysis of the cDNA inserts.

JPET Fast Forward. Published on July 20, 2006 as DOI: 10.1124/jpet.106.105874
This article has not been copyedited and formatted. The final version may differ from this version.

Baculovirus and proteins were produced in ovary cells from *Spodoptera frugiperda* (Sf9) with the BaculoDirect system that utilizes lambda phage integration sites for the recombination reaction with BaculoDirect linear DNA. Once the primary virus was produced, it was amplified and proteins were expressed as described elsewhere (Henderson et al., 2004; Krueger et al., 2005). FAD was added (10 µg/ml) to the cell culture media during protein production to ensure that the level of this essential cofactor would not be limiting. Microsomes were prepared from cells harvested at approximately 96 h post-infection. Protein concentration was determined by the Bradford method, while the FMO content was determined by an HPLC based method (Henderson et al., 2004) that measures the FAD concentration. FAD concentration was corrected for background content. Substrate dependent NADPH oxidation by FMO1 and FMO3 was performed as previously described (Henderson et al., 2004).

DDS- and SMX-Dependent Adduct Formation Catalyzed by Human Recombinant FMO3 and FMO1. An incubation mixture containing FMO3 or FMO1 (50 µg microsomal protein), $MgCl_2$ (3.3 mM), $NADP^+$ (0.065 mM), glucose-6-phosphate (3.3 mM), glucose-6-phosphate dehydrogenase (0.1 U) and DDS or SMX (100 µM) in Tris-glycine buffer (50 mM, pH 9.5) was incubated for 1 h at 37°C. Heat-inactivated FMO3 and FMO1 (90°C for 5 min) was utilized as a negative control to account for non-specific binding of the antisera in this experiment. After 1 h incubation, the reaction mixture was left overnight at 4°C for complete adhesion of protein to the microtiter plate. After 24 h, covalent adducts were determined by an adduct-specific ELISA as described previously (Reilly et al., 2000).

Determination of FMO3 and FMO1 Protein in NHEK. SDS-PAGE, using 10% resolving gels and a Tris-glycine running buffer, was performed according to the method of Laemmli (Laemmli, 1970). Fractionation was carried out using the Criterion Precast Gel Electrophoresis System (Bio-Rad, Hercules, CA.), followed by electrophoretic transfer to a nitrocellulose membrane using the Criterion Blotter (Bio-Rad) (Towbin et al., 1979). Twenty micrograms of microsomal protein were used for each sample of NHEK. Nonspecific binding sites were blocked by overnight incubation at 4°C with 5% nonfat dry milk in Tris-buffered saline (TBS; 25 mM Tris, pH 7.5, 150 mM NaCl). The blots were then incubated for 1 h at room temperature with FMO1 or FMO3 primary antibody diluted 1:5000 in TBS containing 0.5% nonfat dry milk. After extensive washing with several changes of TBS supplemented with 0.1% Tween-20, the blots were incubated for 1 h at room temperature with horseradish peroxidase-conjugated goat anti-rabbit IgG diluted 1:10,000 in TBS containing 0.5% nonfat dry milk. Blots were then washed with several changes of TBS supplemented with 0.1% Tween-20 and processed for detection by enhanced chemiluminescence according to the manufacturer's instructions. The luminescence produced was detected by exposure of Fuji Super RX film (Fisher Scientific, Pittsburgh, PA) and after digitizing the image using a Hewlett Packard 6300C scanner (Boise, ID), the integrated OD of immunoreactive protein bands was determined using a Kodak DC120 digital camera and Digital Science 1D V 3.0 software (New Haven, CT). In all blots, bands corresponding to the protein of interest (FMO1 or FMO3) were identified by reference to the baculovirus-expressed FMO1 and FMO3 and molecular weight standards.

D-NOH Dependent Adduct Formation in Presence of Peroxidase Inhibitor and FMO Competitive Substrate. Protein haptenation following D-NOH exposure to NHEK cells, in the presence or absence of ABH or MMZ was determined. Briefly, NHEK (1 X 10^6 cells) were incubated for 24 h in 50 ml centrifuge tubes containing 10 ml of complete growth medium maintaining the sterile aerobic conditions. Cells were then incubated with D-NOH (100 µM) and immediate addition of the PRX inhibitor (ABH, 5 mM) or the FMO competitive substrate (MMZ, 5 mM). The samples were incubated for 3 h more followed by ELISA analysis for the covalent adducts as described previously (Vyas et al., 2005).

Statistical analysis. Data are presented as mean ± SD. Data were analyzed using SIGMASTAT (San Rafael, CA). Statistical comparisons between two groups were made using either the Student t-test (parametric method) for normalized data or Friedman's rank sum test (nonparametric method) for the data which did not pass the normality test. For comparisons between more than two groups, ANOVA and the Holm-Sidak method for multiple pairwise comparisons were used. A p value <0.05 was accepted as significant.

RESULTS

DDS- and SMX-Dependent Protein Haptenation in the Presence and Absence of Peroxidase Inhibitors in NHEK. We have previously observed that DDS- and SMX-dependent protein haptenation is dose-dependent (Roychowdhury et al., 2005). Various oxidizing enzymes including cytochromes P450, COX, FMOs and PRXs might play an important role in the bioactivation of these drugs in NHEK. In our previous studies, we found that cytochromes P450 and COX do not play major role in the bioactivation of these drugs in NHEK, which led to the focus in this study on the role of PRXs and FMOs in mediating the bioactivation leading to protein haptenation. In order to determine the role of PRX-mediated bioactivation of DDS and SMX, the effect of the PRX inhibitors ABH and KCZ (Kettle et al., 1997; Cornejo et al., 1998) on protein haptenation in NHEK exposed to DDS was evaluated by both confocal microscopy and ELISA. ABH has been generally used for MPO inhibition, but as a hydrazide inhibitor, it also inhibits non-specific PRXs (Ator et al., 1987; Kettle et al., 1995). KCZ, though usually utilized for CYP3A inhibition, has also been reported to inhibit PRXs (Cornejo et al., 1998). For each inhibitor, we utilized the highest inhibitor concentration that did not cause NHEK cytotoxicity. As shown in Fig. 1A and B, ABH and KCZ reduced DDS-dependent protein haptenation in NHEK cells by 35 to 45% and 16 to 24%, respectively. ABH and MMZ caused similar reductions in SMX-dependent protein haptenation (data not shown). Similar results were obtained when inhibitors were added simultaneously with SMX or DDS and incubated for 3 h (data not shown).

Presence of Peroxidases in NHEK. Reduction of covalent adduct formation by PRX inhibitors ABH and KCZ suggested the presence of PRXs in NHEK. To further explore

the presence of PRX activity in NHEK, we utilized the Amplex red reagent for measurement of PRX activity. In the presence of H_2O_2, the Amplex red reagent reacts with PRXs to produce the red-fluorescent oxidation product, resorufin, which has absorption and fluorescence emission maxima of approximately 571 nm and 585 nm, respectively. As shown in Fig. 2, fluorescence increased with increasing amount of NHEK cell lysate, confirming the presence of PRX activity in these cells. Horse radish peroxidase (HRP; 100 µU) was used as a positive control for activity and the ability of ABH (5 mM) to inhibit HRP confirmed the ability of ABH to inhibit PRXs (Fig. 2). Importantly, no measurable increase in fluorescence occurred in a cell free system in the absence of HRP (data not shown).The presence of PRXs in NHEK was also demonstrated by the DAB assay, which gave rise to the brown precipitate expected from the oxidation of DAB (data not shown)**.**

MPO in NHEK. The reduction in protein haptenation by the PRX inhibitors, ABH and KCZ, together with the presence of PRX activity in NHEK, suggested a role for PRXs in DDS and SMX bioactivation. As MPO has been shown to bioactivate arylamines to their hydroxylamine metabolites (Uetrecht et al., 1988), we probed for the presence of MPO in NHEK. Immunoblot analysis (Fig. 3) failed to detect the presence of MPO. In contrast, MPO was readily detected in a myeloid cell line known to express this PRX. The band in NHEK that co-migrated with a band in pure MPO is believed to be that of degradation products due to the heat treatment of these samples. Thus, to probe further for the presence of MPO, we also used RT-PCR amplification and were unable to observe MPO mRNA in NHEK (data not shown). In addition, we also failed to find evidence of MPO-like activity in NHEK using the chlorination assay (data not shown).

LPO in NHEK. The absence of MPO suggested other PRXs may be responsible for DDS and SMX bioactivation. As LPO also has been shown to oxidize arylamines to their nitroso metabolites (Gorlewska-Roberts et al., 2004), we sought to determine the presence of LPO in NHEK. LPO mRNA was readily detected in human salivary glands by RT-PCR amplification (positive control), but was non-detectable in NHEK. The HEK cells also showed the absence of LPO mRNA (negative control) (Figure 4).

TPO in NHEK. The absence of MPO and LPO led us to assess whether or not TPO was present in NHEK. TPO has been shown to oxidize SMX to S-NOH (Gupta et al., 1992). Thus, we probed the presence of TPO in NHEK by immunoblot analysis. TPO was absent in NHEK. Using purified TPO as a positive control, the expected signal at 105 kDa was observed, along with another less intense band at 35 kDa. Neither protein was present in NHEK lysates from three separate patient samples (data not shown).

DDS- and SMX-Dependent Protein Haptenation in the Presence and Absence of FMO Inhibitors in NHEK. The effect of MMZ as a prototypical FMO substrate was used to probe the potential role of this enzyme family on SMX- and/or DDS-dependent protein haptenation in NHEK. The highest concentration of MMZ that did not cause cytotoxicity in NHEK was used. As shown in Fig. 5, MMZ reduced the DDS- and SMX-dependent protein haptenation by 40-50% in NHEK cells when measured by ELISA. Similar results were obtained when MMZ was added simultaneously with SMX or DDS and incubated for 3 h (data not shown). Moreover, using confocal microscopy to detect haptenated proteins (as opposed to ELISA) yielded similar results (data not shown).

DDS- and SMX-Dependent Adduct Formation Catalyzed by Human Recombinant FMO3 and FMO1. To further elucidate the possible role of FMO in metabolizing these

drugs, we studied the *in vitro* bioactivation of DDS and SMX with recombinant FMO enzymes. Both recombinant FMO3 and FMO1 were able to bioactivate DDS and SMX, as shown by the formation of covalent adducts detected by ELISA (Fig. 6). Incubation of DDS with FMO3 showed higher adduct formation compared to FMO1. Heat inactivation of recombinant FMO3 and FMO1 reduced adduct formation by 53 to 60% and 40 to 46%, respectively, compared to non-inactivated enzyme. Despite heat inactivation, significant absorbance was observed. This may be due to incomplete inactivation of the enzymes or non-specific binding of the antisera to the recombinant proteins. Alternatively, there may be some level of chemical-mediated oxidation of DDS that results in protein haptenation in the absence of enzyme activity. Preliminary studies have shown this latter effect occurs to a low degree with BSA (Farley M, Roychowdhury S, Vyas PM, and Svensson CK; personal communication). Significantly, no inhibition of FMO1 or FMO3 catalyzed DDS-dependent protein haptenation was observed when co-incubated with ABH. The optical density representing the protein haptenation of DDS by recombinant FMO3 or FMO1 was 2.83 (±0.18) and 0.54(±0.11), respectively; while the same incubations in the presence of ABH exhibited an optical density of 2.84(±0.11) for FMO3 and 0.55(±0.14) for FMO1.

Analysis of FMO in NHEK. Immunoblot analysis was used to determine the presence of FMO1 and FMO3 in NHEK. Other FMOs were not evaluated as FMO3 and FMO1 are the major FMOs which play a role in the oxidation of various xenobiotics (Chung WG et al., 2000). As shown in Fig. 7, FMO3 was readily detected, while FMO1 was undetectable in NHEK cells. Thus, it appears that only FMO3 is involved in the

observed bioactivation of DDS and SMX to their respective hydroxylamine metabolites in human keratinocytes.

D-NOH Dependent Adduct Formation in Presence of a PRX Inhibitor and an FMO Competitive Substrate. Since the combination of MMZ and ABH were found to inhibit protein haptenation in NHEK to the same level as that seen with either agent alone, we sought to determine if these compounds inhibited sequential steps in the bioactivation leading to protein haptenation. For this reason, we examined protein haptenation following D-NOH exposure in NHEK cells, in the presence or absence of MMZ or ABH. As shown in Fig. 8, ABH was able to reduce the protein haptenation significantly when the cells were treated with D-NOH, indicating a role for PRXs in the conversion of D-NOH to D-NO. MMZ, however, did not reduce the protein haptenation in NHEK exposed to D-NOH.

DISCUSSION

Numerous xenobiotics have been reported to undergo bioactivation to reactive metabolites that cause cellular toxicity (Uetrecht, 1990; Svensson, 2003). Such metabolism to reactive intermediates mostly is mediated through enzymatic or chemical oxidation to form the toxic intermediates capable of binding cellular proteins to form covalent adducts (Lin et al., 2006). Oxidation of SMX and DDS to their arylhydroxylamine and then subsequently to arylnitroso metabolites is believed to be a critical step in their ability to cause CDRs (Naisbitt et al., 1999; Svensson et al., 2001). Various hepatic enzymes, such as the cytochrome P450-dependent monooxygenases, cyclooxygenases and PRXs have been shown to be active in SMX and DDS metabolism (Cribb et al., 1990; Mitra et al., 1995; Goebel et al., 1999; Winter et al., 2000). Though survival of reactive metabolites during transit from liver to skin has not been demonstrated, evidence suggests the presence of the hydroxylamine metabolites of these drugs in plasma and urine after therapeutic doses (Coleman MD et al., 1992; Mitra et al., 1995; Winter et al., 2000). Importantly, the concentration of SMX in skin blisters of subjects receiving this drug achieve 82% of those observed in plasma (Krolicki, 2002). Hence, it has been demonstrated that the parent compound readily penetrates to the epidermal layer of the skin.

We have proposed the bioactivation of such compounds in the epidermal layer of the skin, primarily in keratinocytes (Reilly et al., 2000). The ability of NHEK to metabolize DDS and SMX to their hydroxylamine metabolites with the subsequent formation of cellular protein covalent adducts is consistent with this hypothesis (Reilly et al., 2000; Roychowdhury et al., 2005). Studies to identify the enzyme or enzymes

responsible for DDS and SMX bioactivation in NHEK indicated that neither the CYP450-dependent monooxygenases nor cyclooxygenases are responsible for the observed bioactivation (see companion paper). Thus, we sought to identify other enzymes that are known to oxidize arylamines and might be involved in the bioactivation process in keratinocytes.

PRXs have been shown to bioactivate arylamine drugs resulting in the formation of arylhydroxylamine metabolites (Uetrecht et al., 1988; Cribb et al., 1990). A potential role of PRXs in the bioactivation of DDS and SMX in NHEK was demonstrated by the ability of the general PRX inhibitors, ABH and KCZ (Kettle et al., 1997; Cornejo et al., 1998), to significantly reduce DDS-dependent protein haptenation in NHEK (Fig. 1). While both MPO and LPO have been shown to specifically oxidize arylamine drugs to their arylhydroxylamine metabolites (Uetrecht et al., 1988; Gorlewska-Roberts et al., 2004), no data was found to support the presence of either enzyme in keratinocytes. Using both immunoblotting and RT-PCR amplification, we failed to find evidence for the expression of either MPO protein or mRNA in NHEK (Fig. 3 & 4) and MPO activity was not observed using a chlorination assay. In addition, we found no evidence for LPO mRNA in NHEK.

The lack of evidence for MPO or LPO expression in NHEK, in contrast to the evidence for both general PRX activity and SMX- and DDS-dependent protein haptenation, suggests that other peroxidases may be involved in SMX and DDS bioactivation in these cells. Importantly, TPO has been shown to oxidize SMX to its arylhydroxylamine metabolite *in vitro* (Gupta et al., 1992). This observation, together with evidence for the presence of hypothalamic-pituitary-thyroid axis related genes

expressed in skin, suggests TPO may be a good candidate for the PRX-dependent bioactivation of these drugs in NHEK (Slominski et al., 2002). However, our results showing the absence of TPO in NHEK cells suggests the presence of other oxidizing enzymes which might be inhibited by ABH play a role in the metabolism of these parent drugs.

Other bioactivating enzymes, such as FMOs, are important for the oxidization of arylamine drugs (Cashman, 2000). As previous studies have suggested the presence of FMOs in keratinocytes (Janmohamed et al., 2001), we sought to determine the role of these enzymes in the bioactivation of SMX and DDS in NHEK. Using an FMO substrate, MMZ (Nace et al., 1997), we found a 40-50% reduction in the protein haptenation for both DDS and SMX (Fig. 5). *In vitro* studies demonstrated that recombinant FMO1 and FMO3 can oxidize SMX and DDS, though incubation with FMO3 resulted in a higher level of protein haptenation (Fig. 6). Immunoblot analysis confirmed the presence of FMO3 in these cells, while FMO1 was not detected (Fig. 7). It is possible that the failure to detect this latter FMO is due to the use of low affinity antibodies. While FMO3 (and possibly other unidentified FMO's) seems to be responsible for this bioactivation, our results showing the inability of ABH to inhibit the observed FMO3 activity (data not shown) and the percent inhibition observed with the various inhibitors, suggested that unidentified PRXs or oxidizing enzymes are responsible for between 30 and 40% of SMX and DDS bioactivation, while FMO3 is responsible for 50 to 60% of this activity in keratinocytes.

As we found that combined exposure of NHEK to MMZ and ABH was neither additive nor synergistic in its ability to inhibit protein haptenation upon exposure to SMX

or DDS, we considered the potential that these compounds attenuated sequential steps in the formation of covalent adducts in NHEK. Upon formation, S-NOH and D-NOH can undergo autooxidation leading to their respective nitroso species. It is this latter species that is believed to be the penultimate metabolite for the haptenation of cellular proteins. Our demonstration that ABH but not MMZ attenuates protein haptenation in NHEK exposed to D-NOH suggests that PRXs enhance the oxidation of the arylhydroxylamine to the arylnitroso species (Figure 8A).

The results reported herein, together with our companion study, demonstrate that the relative role of various enzymes in the bioactivation of SMX and DDS differ in keratinocytes compared to liver. While CYP2C9 and CYP3A4 are important enzymes mediating the oxidation of these drugs in liver, they do not play a significant role in keratinocytes. Consistent with this conclusion, previous studies failed to demonstrate a clear association between variant *CYP2C9* alleles and the incidence of sulfonamide-induced CDRs (Pirmohamed et al., 2000).

Taken together, these data indicate that FMO3 plays an important role in the oxidation of arylamines in NHEK, while PRXs play an important role in the subsequent formation of the arylnitroso species. As functional variant *FMO3* alleles have been identified (Koukouritaki and Hines, 2005), it will be important to determine if such variants influence the predisposition of individuals to sulfonamide-induced CDRs. Similarly, environmental and genetic factors that alter the expression of these enzymes should be probed for their potential role in altering the predisposition to these reactions.

ACKNOWLEDGEMENTS

The authors wish to acknowledge the technical assistance of Jamie Schlomann, Sally McCormick and Kevin Leidal in conducting studies for MPO and LPO in support of this project. We also wish to thank the staff of the Central Microscopy Research Facility at The University of Iowa, which is supported by the Office of the Vice President for Research, for their technical assistance.

REFERENCES

Ator MA, David SK and Ortiz de Montellano PR (1987) Structure and catalytic mechanism of horseradish peroxidase. Regiospecific meso alkylation of the prosthetic heme group by alkylhydrazines. *J Biol Chem* **262**:14954-14960.

Borregaard N, Heiple JM, Simons ER and Clark RA (1983) Subcellular localization of the b-cytochrome component of the human neutrophil microbicidal oxidase: translocation during activation. *J Cell Biol* **97**:52-61.

Cashman JR (2000) Human flavin-containing monooxygenase: substrate specificity and role in drug metabolism. *Curr Drug Metab* **1**:181-191.

Chung WG, Park CS, Roh HK, Lee WK and YN C (2000) Oxidation of ranitidine by isozymes of flavin-containing monooxygenase and cytochrome P450. *Jpn J Pharmacol* **84**:213-220.

Coleman MD, Rhodes LE, Scott AK, Verbov JL, Friedmann PS, Breckenridge AM and Park BK (1992) The use of cimetidine to reduce dapsone-dependent methaemoglobinaemia in dermatitis herpetiformis patients. *Br J Clin Pharmacol* **34**:244-249.

Cornejo L, Lopez de Blanc S, Femopase F, Azcurra A, Calamari S, Battellino L and Dorronsoro de Cattoni S (1998) Evolution of saliva and serum components in patients with oral candidosis topically treated with Ketoconazole and Nystatin. *Acta Odontol Latinoam* **11**:15-25.

Cribb AE, Miller M, Tesoro A and Spielberg SP (1990) Peroxidase-dependent oxidation of sulfonamides by monocytes and neutrophils from humans and dogs. *Mol Pharmacol* **38**:744-751.

Cribb AE, Spielberg SP and Griffin GP (1995) N4-hydroxylation of sulfamethoxazole by cytochrome P450 of the cytochrome P4502C subfamily and reduction of sulfamethoxazole hydroxylamine in human and rat hepatic microsomes. *Drug Metab Dispos* **23**:406-414.

Goebel C, Vogel C, Wulferink M, Mittmann S, Sachs B, Schraa S, Abel J, Degen G, Uetrecht J and Gleichmann E (1999) Procainamide, a drug causing lupus, induces prostaglandin H synthase-2 and formation of T cell-sensitizing drug metabolites in mouse macrophages. *Chem Res Toxicol* **12**:488-500.

Gorlewska-Roberts KM, Teitel CH, Lay JJ, Roberts DW and Kadlubar FF (2004) Lactoperoxidase-catalyzed activation of carcinogenic aromatic and heterocyclic amines. *Chem Res Toxicol* **17**:1659-1666.

Gupta A, Eggo MC, Uetrecht JP, Cribb AE, Daneman D, Rieder MJ, Shear NH, Cannon M and Spielberg SP (1992) Drug-induced hypothyroidism: the thyroid as a target organ in hypersensitivity reactions to anticonvulsants and sulfonamides. *Clin Pharmacol Ther* **51**:56-67.

Henderson MC, Krueger SK, Siddens LK, Stevens JF and Williams DE (2004) S-oxygenation of the thioether organophosphate insecticides phorate and disulfoton by human lung flavin-containing monooxygenase 2. *Biochem Pharmacol* **68**:959-967.

Janmohamed A, Dolphin CT, Phillips IR and Shephard EA (2001) Quantification and cellular localization of expression in human skin of genes encoding flavin-containing monooxygenases and cytochromes P450. *Biochem Pharmacol* **62**:777-786.

Kettle AJ, Gedye CA, Hampton MB and Winterbourn CC (1995) Inhibition of myeloperoxidase by benzoic acid hydrazides. *Biochem J* **308 (Pt 2)**:559-563.

Kettle AJ, Gedye CA and Winterbourn CC (1997) Mechanism of inactivation of myeloperoxidase by 4-aminobenzoic acid hydrazide. *Biochem J* **321**:503-508.

Kettle AJ and Winterbourn CC (1994) Assays for the chlorination activity of myeloperoxidase. *Meth Enzymol* **233**:502-512.

Koukouritaki SB and Hines RN (2005) Flavin-containing monooxygenase genetic polymorphism: impact on chemical metabolism and drug development. *Pharmacogenomics* **6**:807-822.

Krolicki A (2002) Skin penetration of sulfamethoxazole and trimethoprim after oral administration. *Ann Acad Med Stetin* **48**:59-73.

Krueger SK, Siddens LK, Henderson MC, Andreasen EA, Tanguay RL, Pereira CB, Cabacungan ET, Hines RN, Ardlie KG and Williams DE (2005) Haplotype and functional analysis of four flavin-containing monooxygenase isoform 2 (FMO2) polymorphisms in Hispanics. *Pharmacogenet Genomics* **15**:245-256.

Laemmli U (1970) Cleavage of structural proteins during the assembly of the head of the bacteriophage T4. *Nature* **227**:680–685.

Lin CY, Boland BC, Lee YJ, Salemi MR, Morin D, Miller LA, Plopper CG and Buckpitt AR (2006) Identification of proteins adducted by reactive metabolites of naphthalene and 1-nitronaphthalene in dissected airways of rhesus macaques. *Proteomics* **6**:972-982.

Mitra AK, Thummel KE, Kalhorn TF, Kharasch ED, Unadkat JD and Slattery JT (1995) Metabolism of dapsone to its hydroxylamine by CYP2E1 in vitro and in vivo. *Clin Pharmacol Ther* **58**:556-566.

Nace CG, Genter MB, Sayre LM and Crofton KM (1997) Effect of methimazole, an FMO substrate and competitive inhibitor, on the neurotoxicity of 3,3'-iminodipropionitrile in male rats. *Fundam Appl Toxicol* **37**:131-140.

Naisbitt DJ, Hough SJ, Gill HJ, Pirmohamed M, Kitteringham NR and Park BK (1999) Cellular disposition of sulphamethoxazole and its metabolites: implications for hypersensitivity. *Br J Pharmacol* **126**:1393-1407.

Nauseef WM, Root RK and Malech HL (1983) Biochemical and immunologic analysis of hereditary myeloperoxidase deficiency. *J Clin Invest* **71**:1297-1307.

Pirmohamed M, Alfirevic A, Vilar J, Stalford A, Wilkins EGL, Sim E and Park BK (2000) Association analysis of drug metabolizing enzyme gene polymorphisms in HIV-positive patients with co-trimoxazole hypersensitivity. *Pharmacogenetics* **10**:705-713.

Reilly TP, Lash LH, Doll MA, Hein D,W Woster PM and Svensson CK (2000) A role for bioactivation and covalent binding within epidermal keratinocytes in sulfonamide-induced cutaneous drug reactions. *J Invest Dermatol* **114**:1164-1173.

Roychowdhury S and Svensson CK (2005) Mechanisms of drug-induced delayed-type hypersensitivity reactions in the skin. *AAPS Journal* **7(4)**:Article 80, DOI: 10.1208/aapsj070480.

Roychowdhury S, Vyas PM, Reilly TP, Gaspari AA and Svensson CK (2005) Characterization of the formation and localization of sulfamethoxazole and

dapsone-associated drug-protein adducts in human epidermal keratinocytes. *J Pharmacol Exp Ther* **314**:43-52.

Slominski A, Wortsman J, Kohn L, Ain KB, Venkataraman G, Pisarchik A, Chung JH, Giuliani C, Thornton M, Slugocki G and Tobin DJ (2002) Expression of hypothalamic-pituitary-thyroid axis related genes in the human skin. *J Invest Dermatol* **119**:1449-1455.

Svensson CK (2003) Do arylhydroxylamine metabolites mediate the idiosyncratic reactions associated with sulfonamides and sulfones? *Chem Res Toxicol* **16**:1034-1043.

Svensson CK, Cowen EW and Gaspari AA (2001) Cutaneous drug reactions. *Pharmacol Rev* **53**:357-379.

Towbin H, Staehelin T and Gordon J (1979) Electrophoretic transfer of proteins from polyacrylamide gels to nitrocellulose sheets: Procedure and some applications. *Proc Natl Acad Sci U S A* **76**:4350–4354.

Tucker KA, Lilly MB, Heck L and Rado TA (1987) Characterization of a new human diploid myeloid leukemia cell line (PLB-985) with granulocytic and monocytic differentiating capacity. *Blood* **70**:372-378.

Uetrecht JP (1990) Drug metabolism by leukocytes and its role in drug-induced lupus and other idiosyncratic drug reactions. *Crit Rev Toxicol* **20**:213-235.

Uetrecht JP (1992) The role of leukocyte-generated reactive metabolites in the pathogenesis of idiosyncratic drug reactions. *Drug Metab Rev* **24**:299-366.

Uetrecht J, Zahid N, Shear NH and Biggar WD (1988) Metabolism of dapsone to a hydroxylamine by human neutrophils and mononuclear cells. *J Pharmacol Exp Ther* **245**:274-279.

Vyas PM, Roychowdhury S and Svensson CK (2006) Role of human cyclooxygenase-2 in the bioactivation of dapsone and sulfamethoxazole. *Drug Metab Dispos* **34**:16-18.

Vyas PM, Roychowdhury S, Woster PM and Svensson CK (2005) Reactive oxygen species generation and its role in the differential cytotoxicity of the arylhydroxylamine metabolites of sulfamethoxazole and dapsone in normal human epidermal keratinocytes. *Biochem Pharmacol* **70**:275-286.

Winter HR, Wang Y and Unadkat JD (2000) CYP 2C8/9 mediate dapsone N-hydroxylation at clinical concentrations of dapsone. *Drug Metab Dispos* **28**:865-868.

FOOTNOTES

This work was supported in part by NIH Grants AI41395 and GM63821 to CKS, HL038650 to DEW and SKK, CA53106 to RNH and Merit Review grant from Department of the Veterans Administration to WMN.

LEGENDS FOR FIGURES

Figure 1. DDS-dependent protein haptenation in NHEK in the presence of peroxidase inhibitors. NHEK were incubated for 3 h in the presence of vehicle (1% DMSO), 5 mM ABH, or 100 µM KCZ. After pre-incubation with inhibitors, cells were incubated for an additional 3 h with 250 µM DDS. **A.** Cells were immunostained followed by confocal imaging and fluorescence intensity of cells exposed to vehicle, DDS or DDS + inhibitors was determined by Image J software. Control represents NHEK incubated with vehicle (1% DMSO) alone. Data presented represent the mean ±SD fluorescence intensity of 9 replicates. **B.** Covalent adducts in cells exposed to vehicle, DDS, or DDS + inhibitors as determined by ELISA. Data represent the mean ±SD optical density of three different experiments having three replicates in each experiment. Data were analyzed statistically using ANOVA with the Holm-Sidak test for multiple pairwise comparisons. $^{*}p< 0.05$ compared to NHEK incubated with vehicle alone, $^{**}p < 0.05$ compared to NHEK incubated with vehicle and DDS, $^{***}p < 0.05$ compared to NHEK incubated with vehicle, DDS and DDS+KCZ.

Figure 2. Presence of Peroxidases in NHEK. Various amounts of NHEK cell lysate supernatant fraction (10 µg – 50 µg) were mixed with 50 µM Amplex red reagent and 1 mM H_2O_2 in a microtiter plate. Following incubation in the dark for 1 h at room temperature, fluorescence was measured using an excitation wavelength of 530 nm and an emission wavelength of 580 nm. Data represent mean ±SD of 6 replicates.

Figure 3. Immunoblot analysis for MPO protein expression in NHEK. Fourth passage NHEK cells were probed for MPO proteins using specific primary and secondary antibodies as described in Materials and Methods. Lane 1 represents

cultured myeloid cell line as a positive control showing the presence of 90 kDa MPO precursor and 59 kDa MPO heavy subunit. Lane 2 represents pure MPO showing the presence of 59 kDa MPO heavy subunit. Lane 3 and Lane 4 represent 10^5 and 8 x 10^5 NHEK cells respectively in which MPO is absent.

Figure 4. Northern blot analysis for LPO mRNA expression in NHEK. Fourth passage NHEK cells were probed for LPO mRNA expression as described in Materials and Methods. Human salivary gland was used as positive control. LPO mRNA was detected as a band at 744 bp. HEK cells were used as negative control.

Figure 5. SMX- and DDS-dependent protein haptenation in NHEK in the presence of an FMO competitive substrate. NHEK were incubated for 3 h in the presence of vehicle (1% DMSO) or 5 mM methimazole (MMZ). After pre-incubation with inhibitor, cells were incubated for an additional 3 h with 250 µM DDS (A) or SMX (B). Covalent adducts were quantified using ELISA as described in Materials and Methods. Data represent the mean ±SD optical density of three different experiments with three replicates in each experiment. Data were compared using ANOVA with the Holm-Sidak test for multiple pairwise comparisons. $^{*}p< 0.05$ compared to NHEK incubated with vehicle alone, $^{**}p < 0.05$ compared to NHEK incubated with vehicle and DDS/SMX.

Figure 6. Human recombinant FMO mediated DDS and SMX adduct formation. Human recombinant FMO3 (represented in A) or FMO1 (represented in B) was incubated with DDS or SMX (100 µM) in an NADPH regenerating system for 1 h at 37°C as mentioned in Materials and Methods. Heat inactivated FMO3 and FMO1 were used as negative controls (represented by gray bars) versus activated FMO3 and FMO1 (represented by black bars). Covalent adducts were determined by an adduct-specific

ELISA as described in Materials and Methods. Data represent mean ±SD of 6 replicates. $^{*}p< 0.05$ compared to the incubation containing heat inactivated FMO3 or FMO1.

Figure 7. FMO3 and FMO1 protein expression in NHEK. Fourth passage NHEK cells were probed for FMO1 and FMO3 proteins using specific primary and secondary antibodies as described in Materials and Methods. A) FMO1 expression: Lane 1-5 represents 25, 100, 250, 350 and 500 fmol of baculovirus-expressed human FMO1 respectively, Lane 6 represents 40 µg and Lane 7 represents 60 µg of NHEK proteins. B) FMO3 expression: Lane 1-5 represents 50, 75, 100, 250 and 500 fmol of baculovirus-expressed human FMO3 respectively, Lane 6 represents 40 µg of NHEK and Lane 7 represents the 60 µg of NHEK proteins.

Figure 8. A. Scheme representing the sequential bioactivation of DDS to D-NO leading to protein haptenation. B. D-NOH dependent protein haptenation in NHEK in the presence of a PRX inhibitor and an FMO competitive substrate. NHEK were incubated with 100 µM D-NOH for 3 h in the presence of 5 mM ABH or 5 mM MMZ. Covalent adducts in cells exposed to vehicle (1% DMSO), D-NOH, or D-NOH + inhibitors were determined by adduct specific ELISA as mentioned in Methods. Data represent the mean ±SD optical density of 6 replicates. Data were analyzed statistically using ANOVA with the Holm-Sidak test for multiple pairwise comparisons. $^{*}p< 0.05$ compared to NHEK incubated with vehicle alone, $^{**}p < 0.05$ compared to NHEK incubated with vehicle, D-NOH and D-NOH+MMZ.

JPET Fast Forward. Published on July 20, 2006 as DOI: 10.1124/jpet.106.105874
This article has not been copyedited and formatted. The final version may differ from this version.

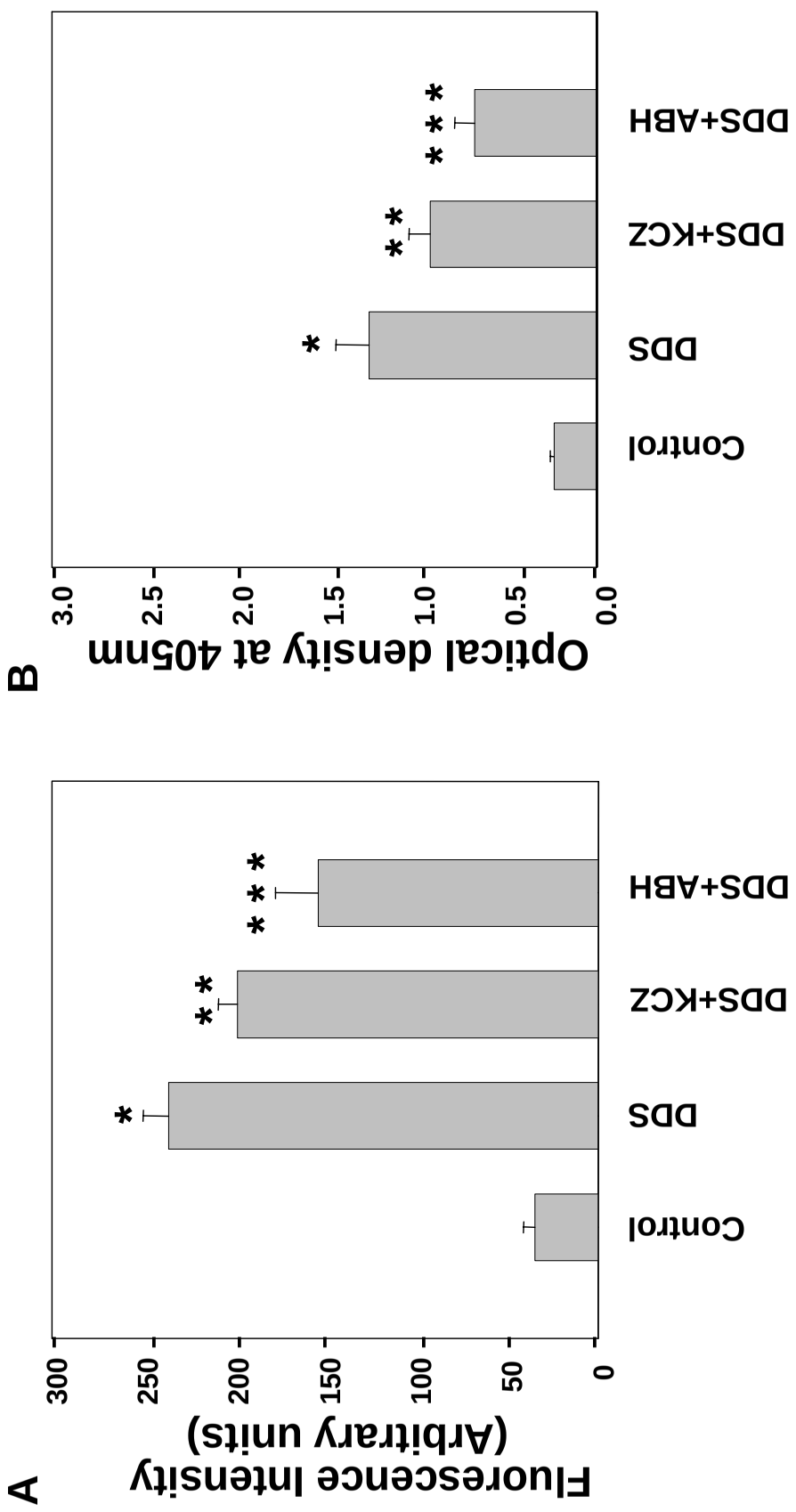

Figure 1

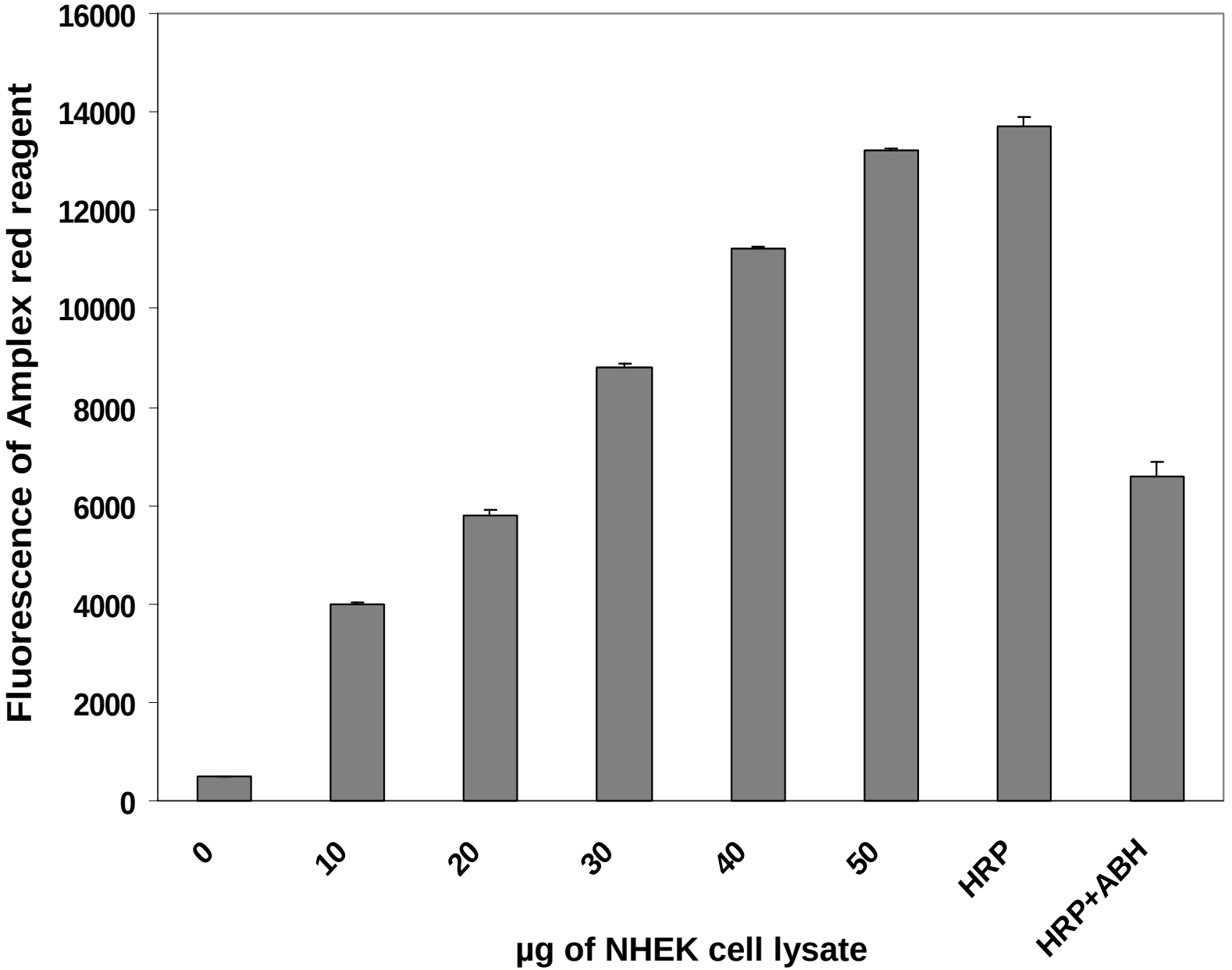

Figure 2

JPET Fast Forward. Published on July 20, 2006 as DOI: 10.1124/jpet.106.105874
This article has not been copyedited and formatted. The final version may differ from this version.

Figure 3

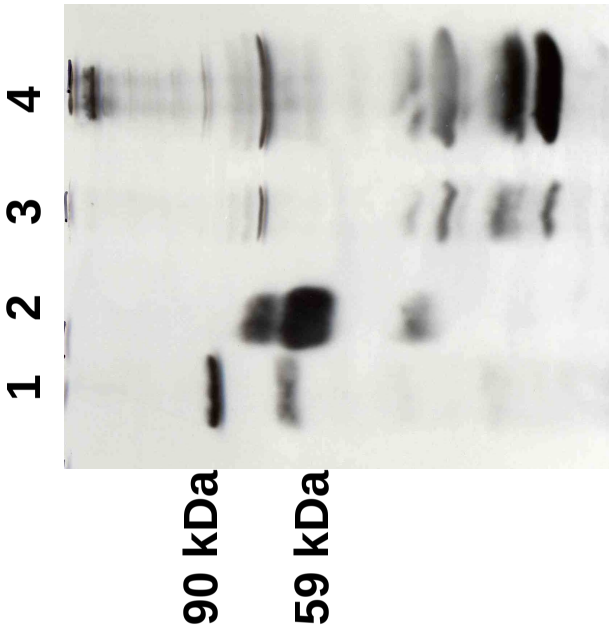

JPET Fast Forward. Published on July 20, 2006 as DOI: 10.1124/jpet.106.105874
This article has not been copyedited and formatted. The final version may differ from this version.

Figure 4

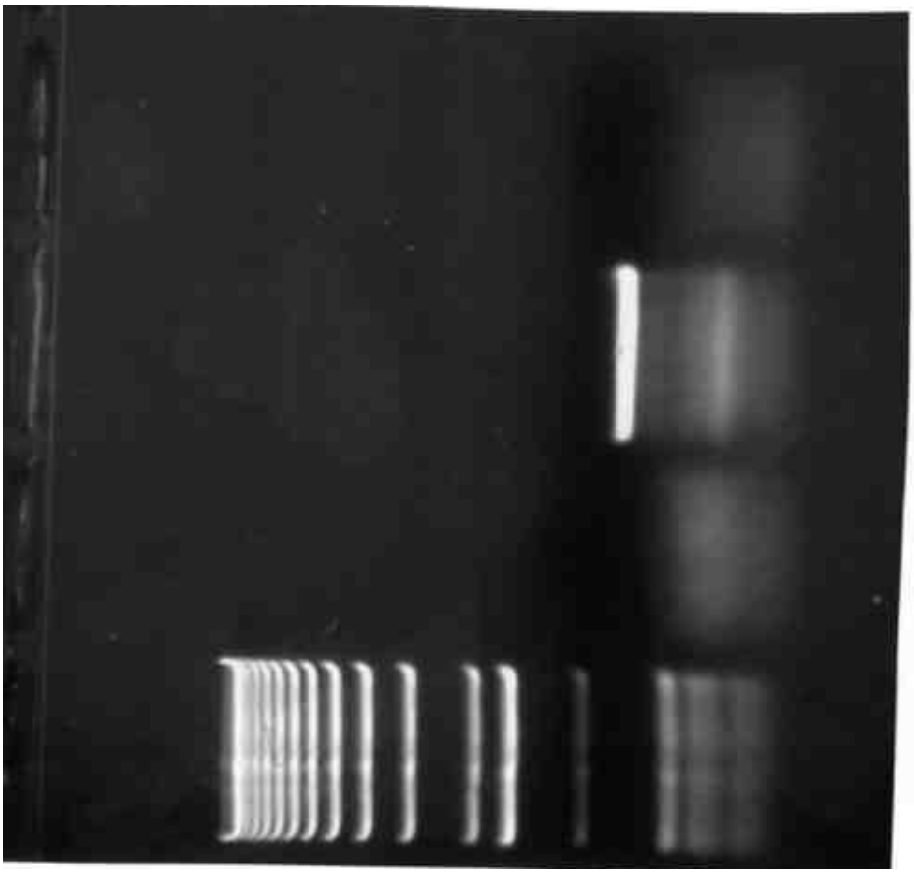

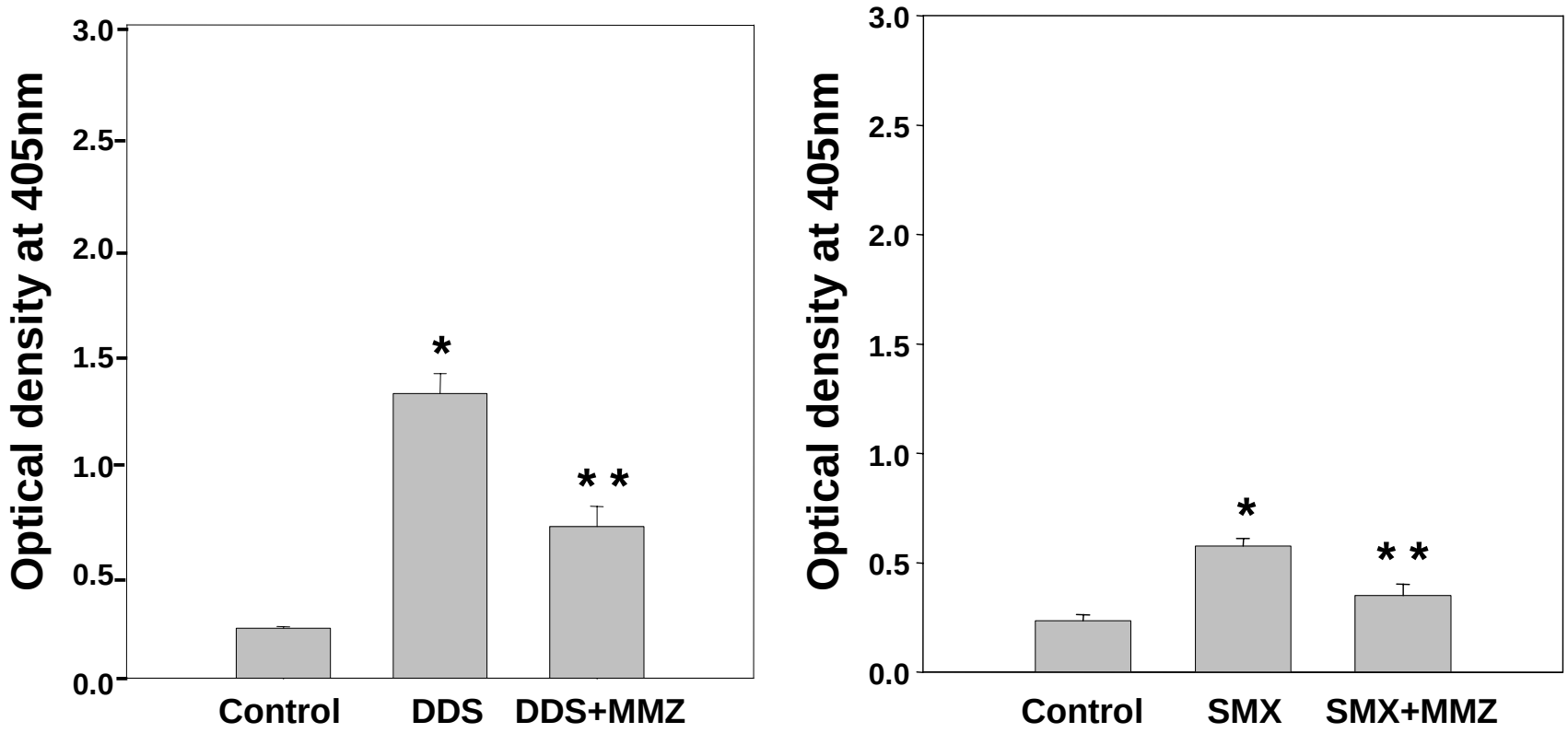

Figure 5

JPET Fast Forward. Published on July 20, 2006 as DOI: 10.1124/jpet.106.105874
This article has not been copyedited and formatted. The final version may differ from this version.

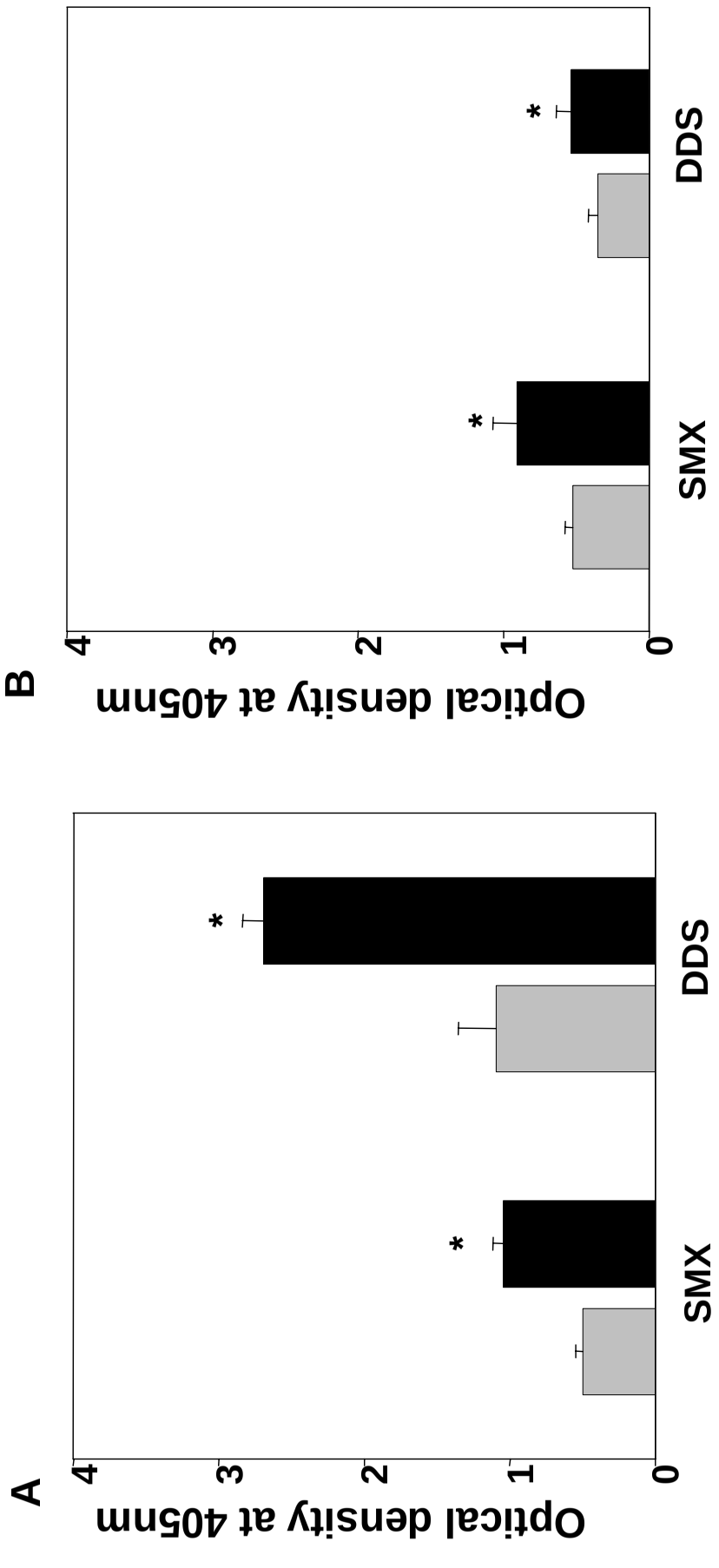

Figure 6

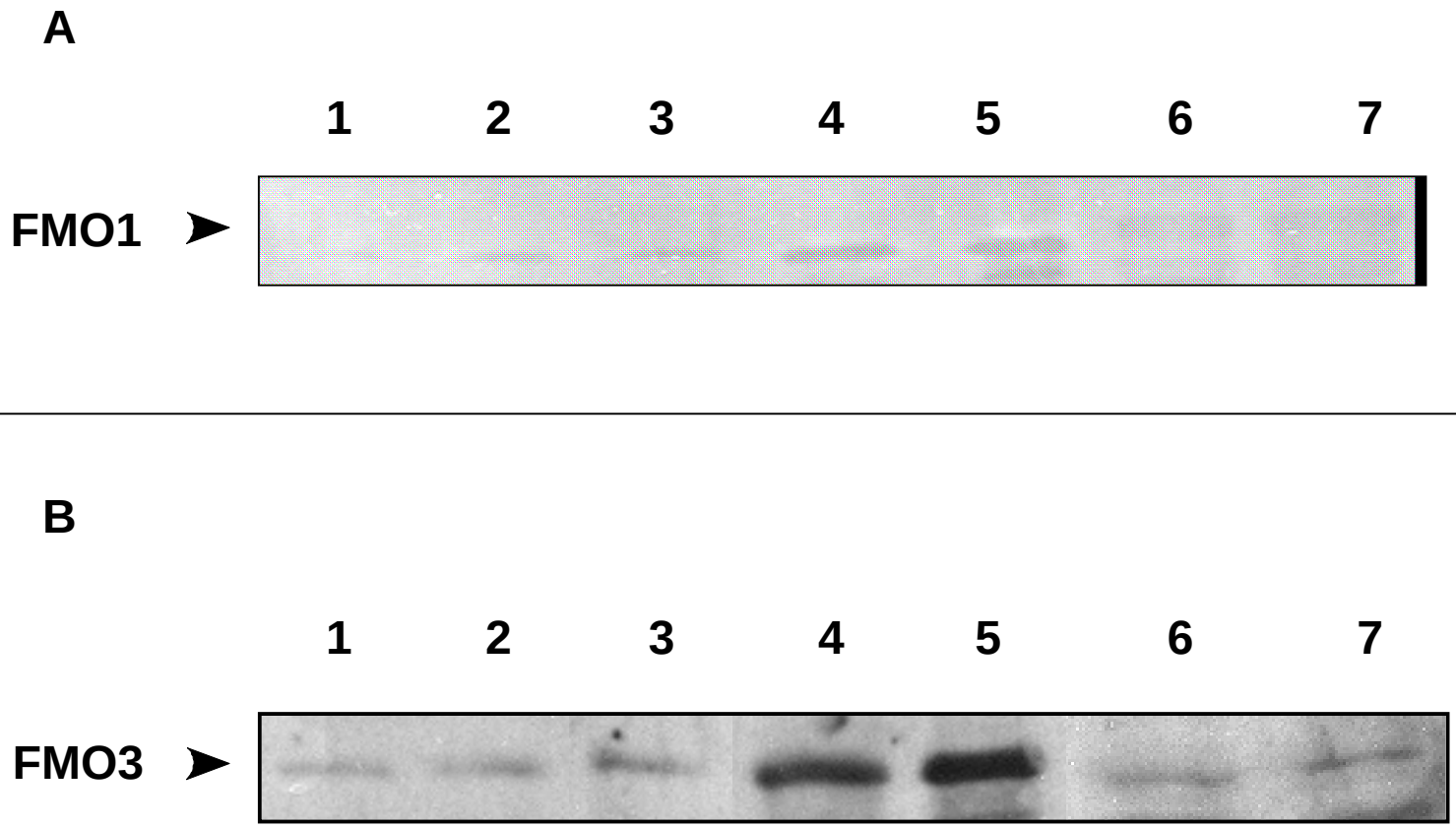

Figure 7

A

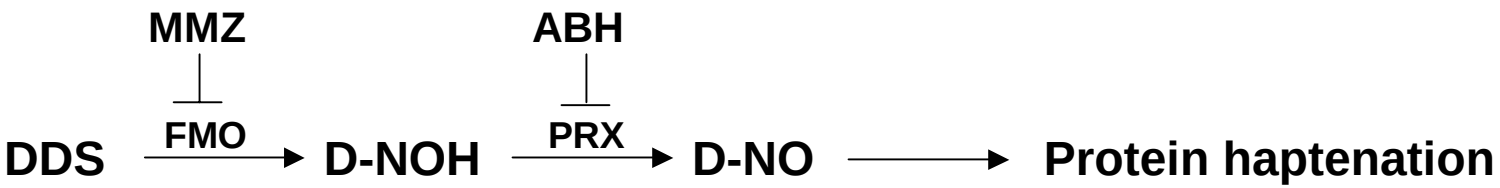

B

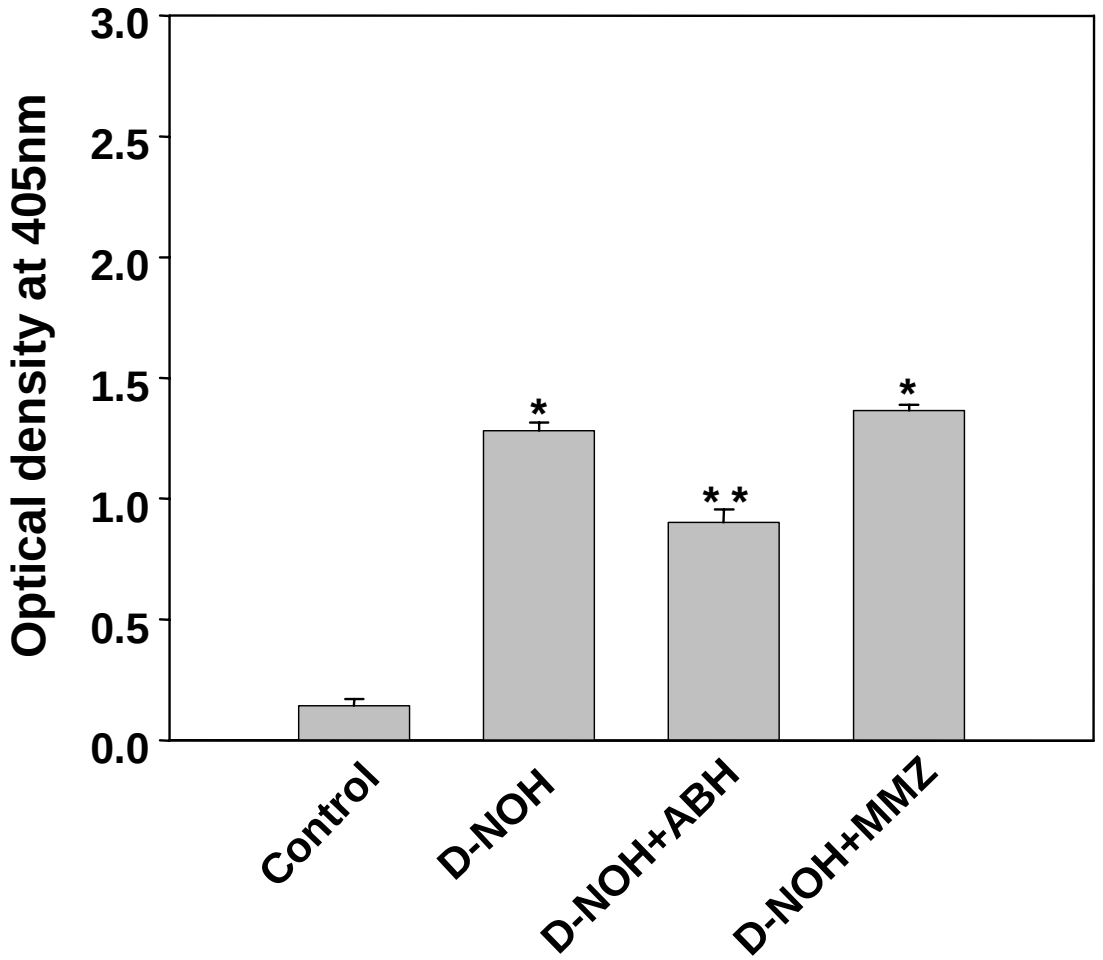

Figure 8